# Superficial and Shroud-like coloration of linen by short laser pulses in the vacuum ultraviolet

Paolo Di Lazzaro,[1,*] Daniele Murra,[1] Enrico Nichelatti,[2]
Antonino Santoni,[1] and Giuseppe Baldacchini[3]

[1]ENEA Research Center of Frascati, Department Applications of Radiation, P.O. Box 65, Frascati 00044, Italy

[2]ENEA Research Center of Casaccia, Department Optical Components Development, via Anguillarese 301, Rome 00123, Italy

[3]Present address: via G. Quattrucci 246, Grottaferrata 00046, Italy

*Corresponding author: paolo.dilazzaro@enea.it

Received 23 July 2012; revised 19 October 2012; accepted 20 October 2012;
posted 22 October 2012 (Doc. ID 173160); published 14 December 2012

We present a survey on five years of experiments of excimer laser irradiation of linen fabrics, seeking a coloration mechanism able to reproduce the microscopic complexity of the body image embedded onto the Shroud of Turin. We achieved a superficial, Shroud-like coloration in a narrow range of irradiation parameters. We also obtained latent coloration that appears after artificial or natural aging of linen following laser irradiations that, at first, did not generate any visible effect. Most importantly, we have recognized photochemical processes that account for both coloration and latent coloration. 

*OCIS codes:* 140.2180, 140.3390, 300.6280, 350.6670.

## 1. Introduction

The front and back images of a scourged man, barely visible on the linen cloth of the Shroud of Turin (see Fig. 1) possess particular physical and chemical characteristics [1] such that nobody was yet able to create an image identical in all its microscopic details, as discussed in a number of papers [2–21].

The inability to replicate the image on the Shroud makes it impossible to formulate a reliable hypothesis on how the body image was made. As a partial justification, scientists complain the Shroud has been seldom accessible. Indeed, the most recent in-depth experimental analysis of the images on the Shroud was carried out in 1978 by the multidisciplinary team of the Shroud of Turin Research Project (STURP). They used the most advanced instruments available at that time, which were supplied by various manufacturers, having a commercial value of over two million dollars. The Shroud was examined by ultraviolet (UV), visible, and infrared spectrometry, x-ray fluorescence spectrometry, microscopy, thermography, pyrolysis mass spectrometry, laser-microprobe Raman analyses, microchemical testing, and fiber sampling [3–13]. These analyses did not find pigments or artist's media on the Shroud, except for some iron oxide particles, micrometer-size cinnabar, and small traces of vermilion (HgS) [13]. However, there is a large body of scientific evidence [8,11,12,16] that the microscopic observations reported in [13] cannot support the Shroud image is a painting. It is likely the microscopic debris particles have been transferred by contact of pigments from artist's copies of the Shroud that have been "sanctified" by pressing the two images together [17].

After years of exhaustive study and data evaluation, the STURP team achieved the following results.

(a) X-ray, fluorescence, and microchemistry results preclude the possibility of paint being used

1559-128X/12/368567-12$15.00/0

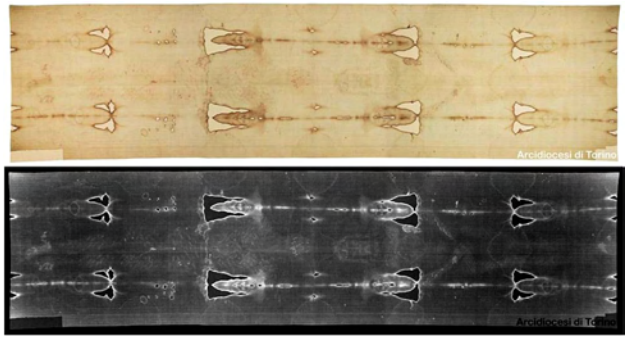

Fig. 1. (Color online) Photograph of the Shroud of Turin and its negative black/white obtained by Jasc software. The image is clearly a negative, not a positive. The dimensions of the Shroud are 441 cm in length and 113 cm in width. From http://www.sindone.org.

as a method for creating the image [7,8,11,12]. UV and infrared evaluation confirm these studies [3,5,6,10]. The body image is not painted or printed.

(b) Both kinetics studies and fluorescence measurements support the image was formed by a low-temperature process. In fact, the temperature was not high enough to change cellulose within the time available for image formation, and no char was produced [12,14]. As a consequence, the body image was not made by a heated bas-relief.

(c) The Shroud's image is superficial as the color resides on the outer surface of the fibers that make up the threads of the cloth [8,11]. Recent measurements on image fibers of the Shroud [19] confirmed that the coloration depth is approximately 200 nm, which corresponds to the thickness of the *primary cell wall* of the linen fiber [22]. In a single linen thread, there are some 200 fibers.

(d) The colored (image) fibers are brittle, show "corroded" surfaces, and are more fragile than uncolored fibers [8,11]. When illuminated by UV light of a lamp, image fibers emit a reduced fluorescent light compared with fibers out of the image [3].

(e) The coloration of the Shroud image was formed by an unknown process that caused oxidation, dehydration, and conjugation of polysaccharide structure of fibers to produce a conjugated carbonyl group as the chromophore [8,11,12]. To some extent, the color is a result of an accelerated aging process of the flax.

(f) The image seen at the macroscopic level is an areal density image. This means shading is not accomplished by varying the color but by varying the number of colored fibers per unit area at the microscopic level [5,9,11,12].

(g) The blood tests positive for human blood, and there is no image on the Shroud beneath bloodstains [12,23]. UV illumination allows observation of typical fluorescence of bilirubin around the main bloodstains [10], which would be consistent with a hemolytic process caused by torture. Independent analyses of forensic pathologist Baima Bollone confirmed STURP's findings [24].

(h) The image fading has three-dimensional (3-D) information of the body encoded in it [14].

All attempts to create a Shroud-like image have failed to reproduce adequately the above characteristics. Some researchers have obtained coloration/images that look similar [5,18,20,21], but no one has created images that match all microscopic and macroscopic characteristics of the Shroud image. The answer to the question of how the image was produced or what produced the image is still unknown. This is the main point of the "mystery of the Shroud." Regardless of the age of the Shroud, either medieval (1260–1390) as dated by radiocarbon test [25,26] or older as it results from other measurements [27], and whatever the importance of historical documents about the existence of the Shroud before 1260 [28,29], the most important question remains the same: how did the image of a man get on the Shroud?

In this paper we approach this unsolved problem, summarizing the main results of experiments carried out at the ENEA Frascati Research Centre aimed at identifying the physical and chemical processes able to generate a Shroud-like coloration.

## 2. Radiative Hypothesis

The results of STURP measurements, briefly summarized in Section 1, have important consequences when seeking possible mechanisms of image formation. Let us discuss some of these consequences, assuming that (according to the STURP conclusion http://www.shroud.com/78conclu.htm) the Shroud covered a man when the body image and blood stains were formed.

- The front and back images do not show the typical deformations of a 3-D body put in contact with a two-dimensional cloth. As a consequence, we deduce that the image was *not* formed by contact with the body. This observation suggests the Shroud was loosely draping the body, that is, it was not wrapped around and in full contact with the whole body. This mode is also supported by the gradations of image brightness that correlate with expected cloth–body distances: in fact, there is a geometrical relationship that corresponds to a body shape and a cloth draping naturally over that shape [14]. Moreover, this "draping mode" is consistent with the lack of image of the body's sides. These considerations, combined with the extreme shallowness of the image color, the absence of pigments, and the subliminal, microscopic complexity of image at the fiber level, make unlikely obtaining a Shroud-like image by contact methods (i.e., by chemicals), either in a modern laboratory [20], or *a fortiori* by a medieval forger. The hypothesis of the medieval forger is also ruled out by the anatomical consistency of blood and serum versus wounds, including the presence of bilirubin, which is invisible to the naked eye. This subliminal feature is only visible by UV fluorescence photography [10] and requires knowledge of anatomy and of forensic medicine [30] not available in the Middle Ages.

- Under the blood there is no image. This means that the blood stains occurred physically on the Shroud before the body image [8,12]. As a consequence, the image was formed after the deposition of the corpse. Moreover, we observe that all the blood stains have sharp outlines and are flawless, and this poses a question if the corpse was removed from the cloth.
- On the Shroud there are no signs of putrefactions, which occur at the orifices about 40 h after death. This means that the image does not depend on putrefaction gases and the corpse was wrapped in the Shroud not longer than two days.

In order to satisfy the conditions posed by these experimental observations, some papers [14,15,18,19] have suggested that an electromagnetic energy incident on a linen fabric could reproduce the main characteristics of the Shroud image, namely the absence of pigments, the shallowness of the coloration, the image in areas not in contact with the body, the gradient of the color, and the absence of image under the blood stains.

The first attempt to reproduce a Shroud-like coloration by electromagnetic energy used a $CO_2$ laser emitting infrared radiation (wavelength $\lambda = 10.6$ μm). These experiments produced an image on a linen fabric similar to the Shroud at macroscopic level [21]. However, microscopic analyses showed a bulky coloration and many fibers carbonized, which are not compatible with the Shroud image [1,12]. In fact, the $CO_2$ infrared radiation excites the vibrational energy levels of the irradiated material, with consequent release of thermal energy, which heats the linen threads in the bulk of the fabric. On the contrary, it is well known that the energy carried by short-wavelength radiation breaks the chemical bonds of the irradiated material without inducing a significant heating (photochemical reaction). Moreover, linen has a molar absorptivity, which increases when decreasing the radiation wavelength. Consequently, the smaller the wavelength, the thinner the material necessary to absorb all the radiation. Therefore, we have chosen the UV radiation to obtain at least two of the main characteristics of the Shroud image: a thin coloration depth and a low-temperature image formation.

### 3. Experimental Results by UV Laser Radiation

Figure 2 shows the setup of the laser irradiations. The laser emits radiation pulses that are focused by a lens onto a linen fabric fixed on a frame. The energy per unit area (fluence) and the power per unit area (intensity) of the laser pulses on linen are varied by changing the surface of linen irradiated, i.e., by moving the fabric with respect to the lens that focuses the laser radiation, as shown in Fig. 2. During the five year irradiation experiments, temperature and relative humidity in the laboratory ranged between 18°C and 25°C and between 50% and 70%, respectively.

When we irradiated linen with our Hercules excimer XeCl laser ($\lambda = 0.308$ μm, single pulse energy 5 J, time duration of each pulse 120 ns), we could not get any coloration. Linens irradiated with high fluence/intensity were carbonized, while at intermediate and low fluence/intensity values we did not observe any change.

Then we irradiated the linen with the radiation emitted by another XeCl laser that emits pulses 4 times shorter and an energy per pulse 12 times smaller than the Hercules laser. The irradiated area was chosen to have the same values of laser fluence incident on linen of the previous irradiations. In this configuration we achieved a permanent coloration of the linen in a narrow range of pulse duration, intensity, number of laser pulses, and time interval between successive pulses.

In summary [31–33], we have shown that the combination of laser parameters necessary to color

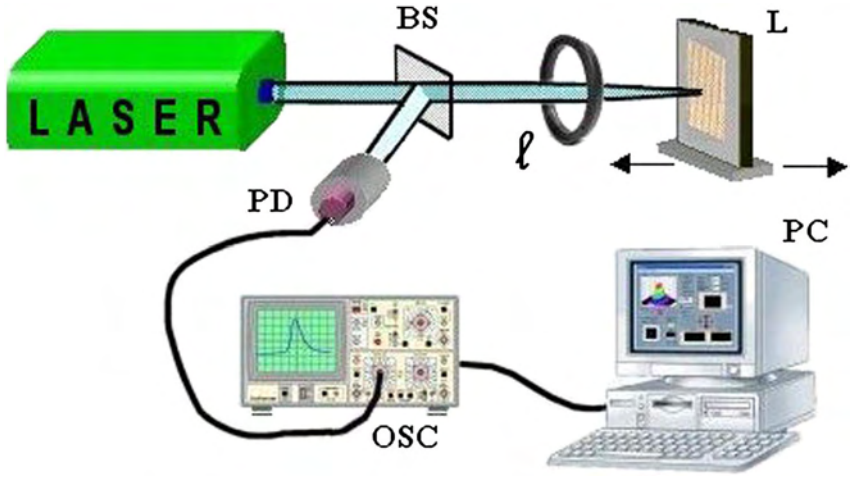


Fig. 2. (Color online) Setup of excimer laser irradiations of linens. The laser pulses are focused by the lens ℓ on the linen fabric L. The laser fluence/intensity on the linen is varied by moving L along the optical axis of the lens. Part of the laser pulse is reflected by the beam splitter BS and monitored by the photodiode PD and the oscilloscope OS connected to a personal computer PC, which processes the data, taking into account the shot-to-shot energy fluctuations. The distance between the XeCl and the ArF excimer lasers and the lens is about 1 m and 25 cm, respectively.

Fig. 3. (Color online) Photomicrograph of the cloth irradiated with 100 XeCl laser pulses. Intensity (fluence) = 16 MW/cm$^2$ (0.5 J/cm$^2$) per pulse.

the linen (the time width of the laser pulses, the intensity/fluence, the number of pulses, the repetition rate) is very narrow. In fact, to obtain the coloring of the flax, UV pulses must be shorter than 50 ns, and small changes of any laser parameter may lead to lack of linen coloration. However, the hue of the color (brown to dark yellow, depending on the intensity and number of laser shots; see Fig. 3) was darker than the yellowish image of the Shroud. The linen coloration was superficial, but the depth of color was still larger than that of the Shroud image. The analysis of the above results suggest that short pulses in the vacuum UV (VUV) would allow a coloration more similar to that of the Shroud. Our choice was the ArF excimer laser.

### 4. Experimental Results by VUV Laser Radiation

The ArF laser ($\lambda = 0.193$ μm, 0.08 J/pulse, 12 ns, 1 Hz) emits radiation in the VUV spectral region with smaller energy and shorter pulse duration than XeCl lasers. Using the same setup shown in Fig. 2, the linen was irradiated in a wide range of laser parameters [34–37] as summarized in Table 1, which reports the observations of the irradiated flax as a function of the number $N$ of consecutive laser pulses, of the spatially averaged fluence $F$ of each laser pulse, of the total fluence $F_T = N \times F$, and of the spatially averaged intensity $I$ of each pulse, defined as follows:

$$F = (1/A) \times \iint_s F(x,y)\mathrm{d}x\mathrm{d}y, \qquad (1)$$

$$F_T = (N/A) \times \iint_s F(x,y)\mathrm{d}x\mathrm{d}y, \qquad (2)$$

where $A$ = area of the flax irradiated by the laser and $F(x,y)$ = fluence at point $x$, $y$ of the transverse area $s$ of the laser beam. An equation analogous to Eq. (1) can be written for $I$.

Table 1 shows that the coloration of linen is proportional to the total laser fluence $F_T$ and is not related to the intensity $I$ nor to the fluence $F$ of each pulse. This surprising behavior is explained assuming that each laser pulse interacts with a linen slightly modified by the previous laser pulse. This cumulative effect becomes visible only when $F_T > 22$ J/cm$^2$, which is the threshold value for coloration. In particular, the yellow color in Fig. 4 is obtained when $F_T \approx (25–27)$J/cm$^2$. When $F_T > 51$ J/cm$^2$, linen is ablated, and when $F_T > 66$ J/cm$^2$, linen is vaporized and holed.

An interesting property of the irradiated linen is the hue of color, which continuously varies from light yellow to yellow–sepia when increasing $F_T$. Then we obtain a fine adjustment of the values of RGB and of the chromatic coordinates (http://en.wikipedia.org/wiki/RGB_color_model) by varying $F_T$, e.g., simply by changing $N$. As an example, let us consider the third row of Table 1. In this case, 50 laser pulses produce a light yellow linen coloration. This means that each laser pulse varies the contrast and the RGB value of the color by a very small amount, equal in average to $1/50 \approx 2\%$, and consequently, we have a very fine control of the chromatic coordinates. In fact, a variation of 2% cannot be appreciated, considering that after 50 pulses (i.e., at 100% of color variation) the color is barely perceptible. Similar arguments can be extended from the second to the seventh row of Table 1.

Equations (1) and (2) show that the $F$ values in Table 1 are averaged over the irradiated area. Because of the nonflat-top spatial profile of the laser fluence, however, the local values of $F(x,y)$ may differ from the average $F$. Consequently, we can observe all the possible effects on the linen in the same area. For example, Fig. 5 shows damaged threads in the linen region at the center of the laser beam [where $F(x,y)$) is higher], while, about 1 mm away, $F(x,y)$ is smaller, and there are yellow colored threads. Near the outer edge of the laser beam, $F(x,y)$ is too small to affect linen threads.

**Table 1. Summary of Main Visual Inspection Results on Linen as a Function of the ArF Laser Irradiation Parameters**

| $N$ | $I$ (MW/cm$^2$/pulse) | $F$ (J/cm$^2$/pulse) | $F_T$ (J/cm$^2$) | Macroscopic Findings on Linen |
|---|---|---|---|---|
| 30 | 35 | 0.420 | 12.6 | No change |
| 100 | 14 | 0.168 | 16.8 | Coloration only visible at grazing incidence |
| 50 | 36 | 0.432 | 21.6 | Light yellowing |
| 200 | 10.5 | 0.126 | 25.2 | Yellow color |
| 200 | 11.2 | 0.134 | 26.8 | Yellow color |
| 402 | 6.6 | 0.073 | 29.3 | Yellow–sepia |
| 600 | 6 | 0.066 | 39.6 | Yellow–sepia |
| 500 | 13.3 | 0.146 | 73.0 | Ablation |

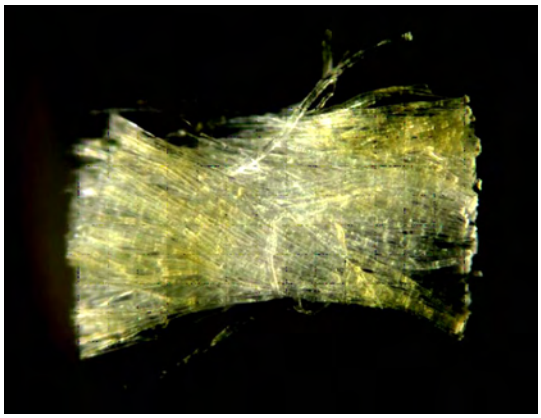

Fig. 4. (Color online) Photomicrograph of a warp thread of flax irradiated with ArF laser at a total laser fluence $F_T = 26.4\ \mathrm{J/cm^2}$. The thread was crushed with forceps to separate the fibers and highlight their yellow color. At the center of the thread, there is a uncolored zone due to a weft thread that shadowed the laser radiation [36].


Fig. 5. (Color online) Area of the linen irradiated by the ArF laser beam shows different characteristics that depend on the local values of $F(x,y)$. (1) Colored area, (2) ablated area, and (3) area irradiated below the threshold for coloration [36].

Concerning the thickness of coloration, photomicrographs [an example is shown in Fig. 6(a)] show coloration depths ranging between 7 and 26 μm in threads irradiated with different intensities [35]. This is a range of thicknesses 11 to 3 times thinner than the coloration depth achieved by the radiation at $\lambda = 0.308$ μm; see Fig. 6(b) [32,33]. As the threads of our linen fabric have an average diameter of 300 μm, we deduce that the light at $\lambda = 0.193$ μm penetrates 2% to 9% of the diameter of the linen yarn, depending on the specific conditions of irradiation.

Among the analyzed fibers, we found one showing a colorless inner part (see Fig. 7), and in this case it is possible the color affects only the outermost film of the same fiber, the so-called *primary cell wall*, which is about 0.2 μm thick. This result is close to the thinnest coloration depth observed in the Shroud image fibers [19].

## 5. Latent Coloration

We cut half of the laser spot on linen irradiated with $F_T = 16\ \mathrm{J/cm^2}$, i.e., below the threshold for coloration; see Table 1. As a consequence, the irradiated linen did not appear colored. We then heated one of the two parts by an iron at a temperature of 190 ± 10° C for 10 s, and a coloration appeared immediately after heating. Figure 8 shows that the heating process, which simulates aging, colors only the surface irradiated below threshold and does not color the nonirradiated area. Moreover, when heating linen irradiated in the conditions of the first row of Table 1, no latent coloration is observed after heating. That is, in the latter case, we are below the threshold for latent coloration. Therefore, we deduce that the range for obtaining a latent coloration is $F_T \approx (13\text{–}20)\mathrm{J/cm^2}$. Finally, when heating a colored linen, we observe a more evident coloration, with a stronger contrast with respect to the surrounding, nonirradiated area.

Using the short-pulse XeCl laser, we have obtained a latent coloration similar to that of Fig. 8, which appeared after a natural aging of more than one year, maintaining the linen at room temperature in a dark environment [32].

The importance of these results is twofold. On one hand, there is the scientific interest of UV and VUV light that breaks chemical bonds in a way to favor the oxidation and dehydrating effect of heat (aging), finally resulting in linen coloration. This dual mechanism will be discussed in Section 8.A. On the other hand, there is the interest of historians,

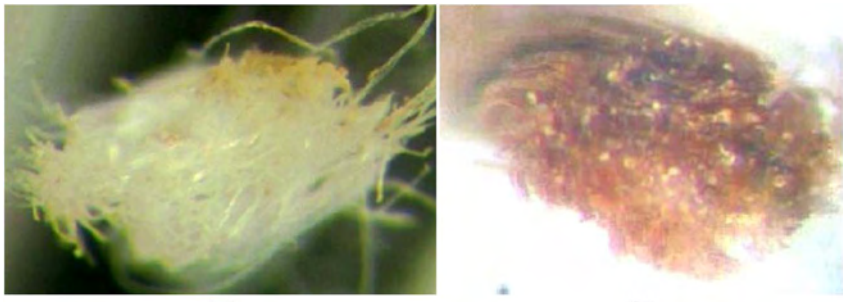


Fig. 6. (Color online) Photomicrographs of the cross section of two linen threads, irradiated by (a) ArF and (b) XeCl laser beams, respectively, "from top" of photos. In (a) VUV colors a very thin topmost part of the thread, corresponding to few fibers. In (b) UV colors more than one half of the section of the thread. Both threads have an average diameter of 300 μm [35].

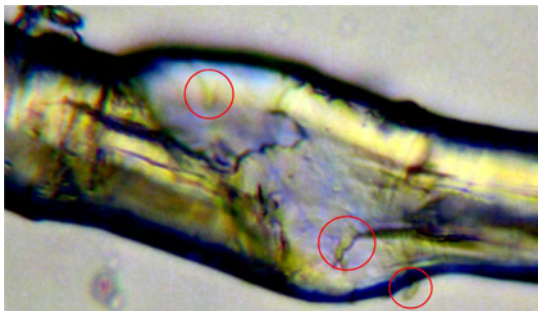

Fig. 7. (Color online) Microscope image of a single linen fiber colored after ArF laser irradiation. The mechanical damage in the central part allows observation of small broken pieces of colored primary cell wall (see inside circles) on a colorless inner part of the fiber. The average diameter of the fiber is 20 μm.

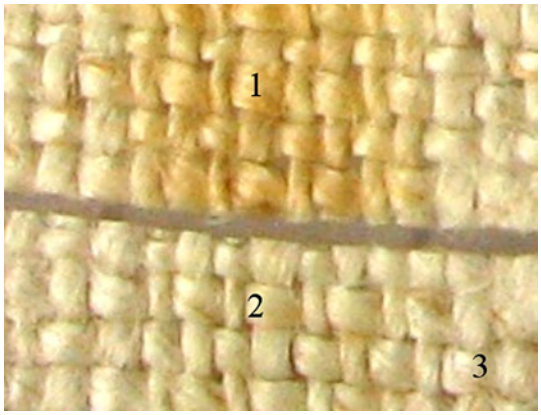


Fig. 8. (Color online) Linen fabric cut after irradiation below threshold for coloration. (1) Irradiated area after heating. (2) Irradiated area, not heated. (3) Nonirradiated area. Latent coloration is limited to the area of the linen irradiated below threshold and appears only after artificial aging of the upper part of irradiated linen [36].

attracted by the possibility that, whatever may have caused the Shroud image, the coloration may not have been immediately visible, i.e., it may have "developed" over time.

## 6. Fluorescence by UV Illumination

Linen fabrics emit blue fluorescence when illuminated by UV light. However, spectroscopy measurements show the Shroud fibers of the image emit only 50% of fluorescent light emitted by fibers out of the image [3]. This quenched fluorescence is one of the most peculiar characteristics of the Shroud image.

Figure 9(a) shows a linen fabric after ArF laser irradiation when illuminated with a UV lamp. The area irradiated by the laser emits a much smaller blue fluorescence with respect to the linen fabric. This result suggests that the VUV radiation of the laser has changed the electronic structure of the cellulose to reduce the typical fluorescence of the linen. The image threads of the Shroud behave the same way.

Similar to the laser coloring process, the quenched fluorescence of the irradiated threads takes place only in a narrow range of the irradiation parameters. For example, Fig. 9(b) shows that laser pulses having a doughnut-shaped $F(x,y)$ profile inhibit the fluorescence only in an ellipsoidal ring irradiated by the correct value of $F_T$. Outside this annular region, $F_T$ is too weak to inhibit the fluorescence. This means that the fluorescence induced by UV provides accurate and selective information on the local intensity profile able to generate a Shroud-like coloration.

## 7. Further Experiments

### A. How Much Different is Our Linen from the Shroud?

In our experiments, one wonders about the differences between our linen fabric and the linen of the Shroud, besides the age. As our experiments involve photons and optics, we measured some additional optical characteristics of our linen to be compared with the linen of the Shroud. We used a Perkin–Elmer Lambda 950 spectrophotometer equipped with a 15 cm diameter integrating sphere [38]. The interior of the sphere is covered with a plastic material known as Spectralon, whose characteristics of reflection are almost 100% Lambertian and constant over the whole spectrum between UV and visible. Additionally, this instrument has an internal calibration of the Spectralon, which allows the direct measurement of the absolute reflectance spectra. We measured the hemispherical absolute spectral reflectance $R(\lambda)$ (i.e., the percentage of light reflected by our linen with respect to the incident light), and the results are shown in Fig. 10, together with the spectral reflectance measured on the Shroud as

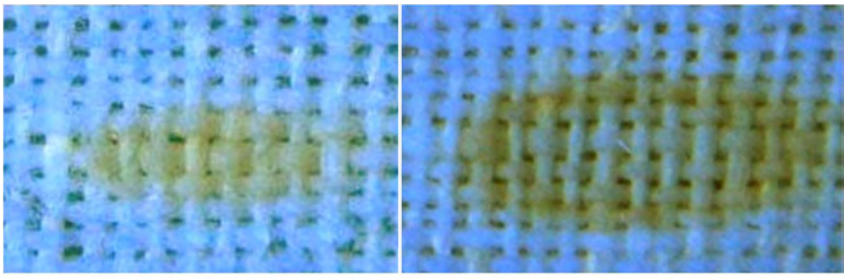


Fig. 9. (Color online) Blue fluorescence induced by UV lamp on linen after irradiation with ArF laser. (a) In the working point of the third row of Table 1. The irradiated area shows a reduced fluorescence. (b) By using a laser beam having a "holed" spatial profile of the intensity. In this case the fluorescence reduction is not uniform over the whole laser spot.

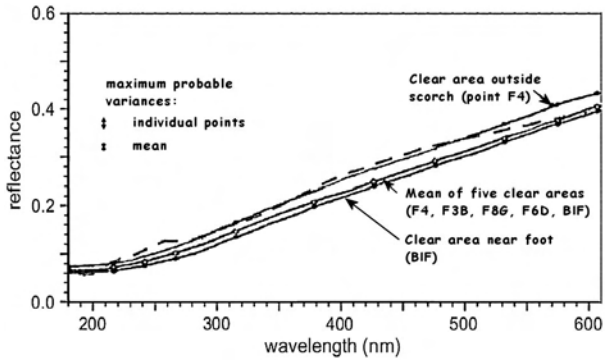


Fig. 10. The solid curves show the absolute reflectance of the linen of the Shroud in areas of no image as a function of the wavelength [3]. The dashed curve shows the absolute hemispherical reflectance of the linen used in our experiments [35].

reported in [3]. Figure 10 shows a strong similarity of our linen with respect to the Shroud. We note a small difference in the spectral region between 520 and 600 nm, showing our linen is less yellowish than the Shroud, possibly because of the different age. Most important, the absolute reflectance of the two linens at the laser wavelengths we used, 193 and 308 nm, is almost the same. Thus, when irradiated in the UV and VUV, our linen behaves like the linen of the Shroud.

Using the same spectrophotometer, we measured the hemispherical transmittance $T(\lambda)$ of the linen (i.e., the light transmitted by our linen with respect to the incident light) as a function of wavelength. Then we can deduce the spectral absorbance $A(\lambda)$ as follows:

$$A(\lambda) = 1 - R(\lambda) - T(\lambda), \tag{3}$$

that is, $A(\lambda)$ is the amount of light absorbed by linen as a function of wavelength. The results are shown in Fig. 11.

### B. Can UV Laser Radiation Make Linens Older?

The process of dehydrative oxidation that produces the Shroud image can be considered a kind of premature aging of linen [8]. To check if the excimer laser irradiation produces a similar aging effect, we observed some linen fibers placed between crossed polarizers in a petrographic microscope to detect changes induced by laser irradiation in the crystal structure of the fibers. The petrographic microscope allows us to observe a pattern of isochromatic lines that depend on age of the sample, mechanical stress, and presence of defects. When the fibers are aligned to the axis of polarization of the analyzer, we see a dark image: in this case the fibers are placed "to extinction," and there is no birefringence. If a part of the fiber aligned to extinction is damaged, it becomes birefringent and appears bright because damaged regions have a different crystalline orientation than the fiber. Figure 12 shows a partially irradiated fiber of linen immersed in oil as observed in cross polarization to identify the stressed regions of the fiber. The nonirradiated region has the usual aspect of a recent linen. In contrast, the irradiated (colored) region of the fiber shows bright spots and tracks corresponding to stressed areas coupled with high-fragility zones. The dehydration of the fiber cellulose is in fact associated with an increment of the fiber fractures pointed out by birefringence at the location of the defects.

A similar behavior is observed on old linen fibers like those used to wrap Egyptian mummies. We can therefore infer that short and high-intensity UV pulses change the crystalline structure of cellulose in a similar manner as aging and low-intensity radiation (radon, natural radioactivity, secondary particles from cosmic rays) accumulated in a long-term period do.

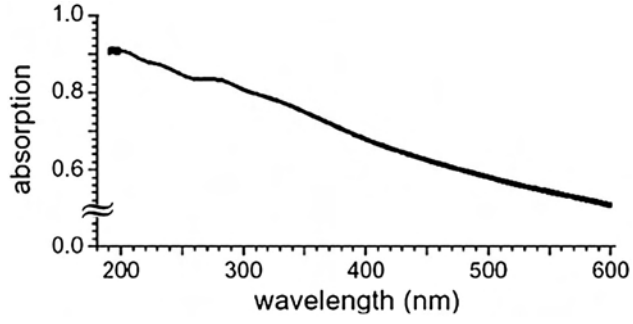


Fig. 11. Plot of the absolute value of the absorbance of the linen versus the wavelength, according to our experimental values inserted in Eq. (3). The thickness of the plot gives the error associated to the measurement.

### C. Is the Coloration Induced by Excimer Laser Irradiation a Photochemical or a Thermal Effect?

In order to verify whether the UV and VUV light interacts with the linen by photochemical or thermal processes, we used the infrared camera ThermoShot F30 (http://www.nec-avio.co.jp/en/products/ir-thermo/pdf/catalog-f30-e.pdf) equipped with microbolometers sensitive in the spectral range 8–13 μm. This camera is able to measure the surface temperature of objects with the uncertainty of ±0.2°C.

The camera was aligned in front of the linen during laser irradiation, monitoring in real time the

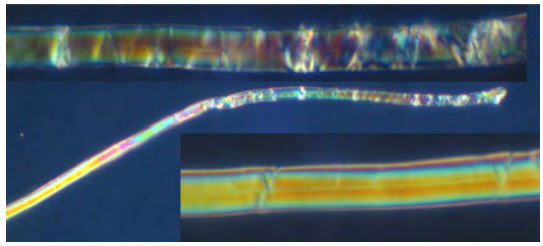

Fig. 12. (Color online) Petrographic microscope observation of a linen fiber. In the middle there is a partly colored fiber of linen in oil 1.515 between crossed polarizers. The left part of the fiber is the nonirradiated region, which is enlarged in the inset below. On the right there is the region irradiated by XeCl laser, enlarged in the inset above. From [32].

temperature of the whole linen fabric as shown in Figs. 13(a) and 13(b). During laser irradiations, the room temperature was between 20°C and 21°C, and the linen region irradiated by the UV XeCl laser was heated up to 33°C, while the linen irradiated by the VUV ArF laser was heated up to 25°C. It is known that thermal effects can color the linen only when the linen temperature approaches 200°C [11], and we can conclude that excimer laser coloration is a photochemical process that does not involve significant thermal effects.

## 8. Analysis of Results

Our results show that excimer lasers are powerful tools to simulate the physical and chemical processes that might have caused the peculiar coloration of the Shroud image. In order to gain a deeper insight into these processes, we need to detail some chemical and physical properties of linen fabrics and of the excimer lasers.

### A. Chemical Processes

Each thread of linen consists of about 200 fibers, rodlike structures with an average length of 30 mm and average diameter of 20 μm. Each linen fiber has an inner part (the secondary cell wall) of cellulose, and a thin (0.2 μm) outer skin (the primary cell wall) composed of hemicellulose (predominantly xyloglucan) bound with pectin to cellulose [22]. Let us recall that hemicellulose is a polysaccharide similar to cellulose, but it consists of shorter chains (500–3000 sugar units) as opposed to 7000–15,000 glucose molecules per polymer seen in cellulose. While cellulose is crystalline, hemicellulose has an amorphous structure with little strength. To some extent, hemicellulose can be considered a degraded form of cellulose.

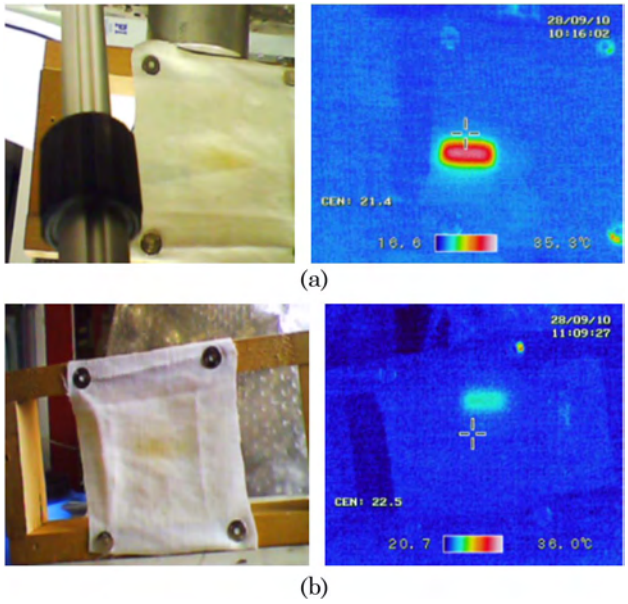


Fig. 13. (Color online) (a) (Left) Photo of the linen during XeCl laser irradiation. (Right) Same picture seen in infrared light. The color scale at the bottom shows that the warmest region of the linen (in the middle of the laser spot) reaches 33°C, while the nonirradiated area is at the room temperature of 20°C. (b) (Left) Photo of the linen during ArF laser irradiation. (Right) Same frame seen in infrared light. The color scale reveals that the warmest area of the irradiated linen is at 25°C, while the nonirradiated area is at the room temperature of 21°C.

The STURP results show the image chromophore is a conjugated carbonyl produced in the polysaccharide structure of fibers by a dehydrative oxidation process [8,11,12,39]. The color of the Shroud image is a result of an accelerated aging process of the linen, similar to the yellowing of ancient papers [40]. Figure 14 shows two different chemical paths possibly involved in the formation of the image on the Shroud.

The different thickness of coloration obtained with the XeCl and ArF lasers (see Fig. 6 and Sections 3 and 4) may be due to the different $\lambda$, respectively emitted. In fact, the shorter the wavelength, the larger the energy absorbed per unit volume. However, Fig. 11 shows there is only a difference of 11% between the flax absorption at 0.193 μm and at 0.308 μm [34,35]. As a consequence, we must find an additional mechanism to explain the different penetration depth of light in the fibers and the different hue of color, i.e., yellow after ArF laser irradiation at 0.193 μm and light brown after XeCl laser irradiation at 0.308 μm; see Figs. 3 and 4. This additional mechanism could be promoted by the absorption band below 0.2 μm of alkene groups (—C═C—) [41] typical of degraded cellulose and of organic impurities of the primary cell wall of linen fibers. The VUV absorption of these groups may trigger a reaction chain that leads to photo-oxidation (aging) and to new alkenes and carbonyl groups. After a proper irradiation dose, new conjugated C═C and C═O groups are formed, increasing delocalization and thus shifting the absorption band to longer wavelengths in the blue–green region of the visible spectrum, to finally produce the yellowish Shroud-like coloration shown in Figs. 4, 5, 6(a), and 7. Note that the XeCl wavelength is too long to fit in the absorption band of alkenes, so that it is not able to start the many-step process schematized in Fig. 14.

In this frame, the formation of latent images described in Section 5 can be explained by oxidation and dehydration of the cellulose (caused by heat or by natural aging) amending the new chemical bonds induced by laser irradiation, thus facilitating the formation of conjugated unsaturated structures that are an essential part of the chemical transitions in Fig. 14. The synergy between heat and UV light is detailed in [42], showing how the process initiated by exposure to UV radiation is accelerated and reinforced by heat.

### B. Physical Processes

Let us consider the different role of laser intensity and fluence in the coloration of the linen. We showed in Section 3 that XeCl laser pulses having the same fluence but different pulse durations (i.e., different intensities) produce different colorations. This

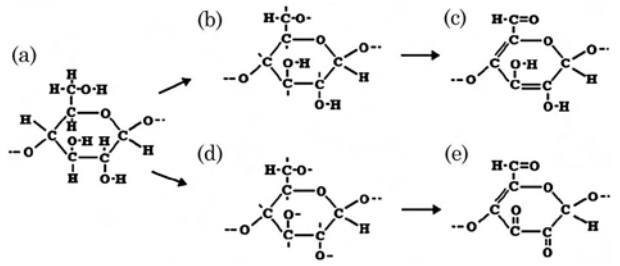


Fig. 14. (a) Main molecular structure common to both cellulose and hemicellulose. There are two possible transitions (*a*) → (*b*) → (*c*) and (*a*) → (*d*) → (*e*) that generate chromophores after oxidation and dehydration. The C═C and C═O double bonds in (c) and (e) act as chromophores and are responsible for the yellow color of the fibers of image on the Shroud of Turin.

suggests that the intensity is the key parameter. However, Table 1 shows that consecutive laser pulses sum their effects, and the key parameter is $F_T$, that is, the number of photons per unit area. This apparent dichotomy evidences that we are observing a complex photochemical process, where intensity and fluence play in turn a dominant role, depending on the duration of the pulses, the number of photons per unit area, and the number and repetition rate of laser pulses.

Let us now analyze why it is so difficult to get a coloration limited to the primary cell wall of flax fibers (see Fig. 7). As mentioned in Section 4, the fluence/intensity spatial profile of the excimer laser beam is not uniform, showing high-frequency spatial fluctuations, which can be detected and measured by a CCD camera with high spatial resolution; see Fig. 15.

The fluctuations in Fig. 15 have an irregular period, with gradients of intensity/fluence up to 350 MW/cm$^2$ per centimeter (4 J/cm$^2$ per centimeter). The value of laser intensity (fluence) incident on two points of the linen at, say, 1 mm distance can vary up to 35 MW/cm$^2$ (0.4 J/cm$^2$). The huge value of the intensity/fluence gradient can explain why it is possible to get the "right" value of intensity for submicrometer coloration only in a very limited area, which is difficult to be found by photomicrographs.

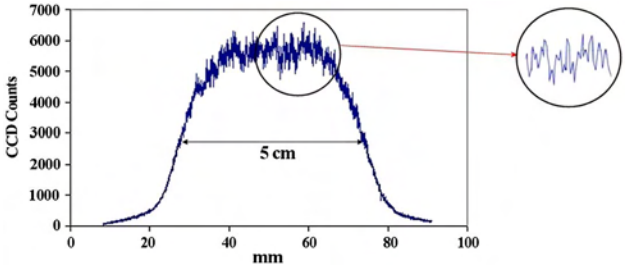


Fig. 15. (Color online) One-dimensional intensity/fluence profile of our laser beam measured by a CCD camera Andor Model DV-430UV, with a 22 μm single-pixel resolution. The inset shows an enlargement of the high-frequency spatial fluctuations. Note that the contribution of CCD noise to the spatial fluctuations on the plateau is negligible, of about $4 \times 10^{-3}$.

As mentioned in Section 1, point (f), the shading of the Shroud image is not accomplished by varying the color but by varying the number of colored fibers per unit area [5,12]. In addition, the image area has a discontinuous distribution of color along the threads of the Shroud [9]. Some of these features can be found in our irradiated linens; see, e.g., Fig. 16, which shows colored fibers next to uncolored ones in the same thread.

However, we did not fully achieved a "half-tone effect" comparable with that observed on the Shroud [5,12]. In principle, it would be possible to replicate exactly this characteristic by laser pulses having a spatial intensity distribution "sawtoothlike" with variable period. This distribution can be achieved by state-of-the-art diffractive optics that arbitrarily modulate the spatial distribution of laser beams [43].

## 9. Summary, Consequences, and Remarks

In this paper, we summarized the current state of knowledge on the Shroud image and the reasons of the difficulty to create an image that matches its peculiar superficiality and chemistry at the microscopic level. After countless attempts, the inability to replicate the image on the Shroud prevents the formulation of a reliable hypothesis on the process of the image formation. Because of these scientific and technological difficulties, the hypothesis of a medieval forger does not seem reasonable. We then summarized the experiments done at the ENEA Research Center of Frascati, which have demonstrated the ability of VUV light pulses lasting few nanoseconds to generate a Shroud-like coloration on linen that matches many (although not all) characteristics of the Shroud image. By the way, the ability of VUV light to generate a Shroud-like coloration helps to clarify the controversy between two scientists of the STURP team: Jackson, who foresaw the possibility of coloring flax by VUV radiation [15], and Rogers, who believed that laser pulses would have heated and vaporized flax, without any coloration effect [44]. Rogers' opinion was based on the

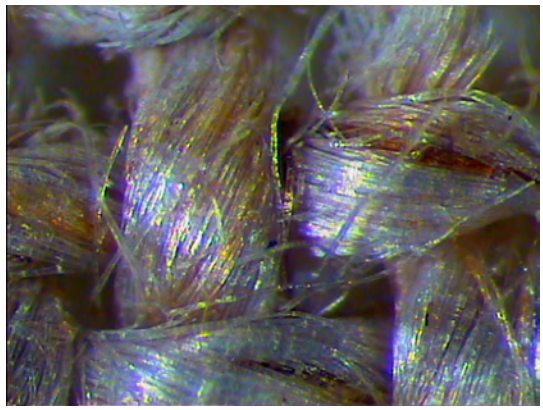

Fig. 16. (Color online) Photomicrograph of linen threads after ArF laser irradiation. Single colored fibers are visible next to uncolored fibers, like in the Shroud image.

failure of experiments made at Los Alamos using excimer lasers, but our results demonstrate that their failure was due to parameters (e.g., laser pulse width) outside the narrow range of values able to generate the permanent linen coloration.

Let us summarize in the following the main results we achieved.

I. We obtained a linen coloration only in a narrow range of laser parameters. In particular, the temporal duration of the single laser pulse must be shorter than 50 ns [31,32]. While a short laser pulse width is necessary for obtaining a coloration, the VUV laser spectrum allows a coloration limited to the outer surface of the threads.

II. The most interesting results were obtained with VUV light. The permanent linen coloration is a threshold effect, i.e., the color is obtained only when $F_T > 22$ J/cm$^2$; see Table 1. When the $F_T$ value is above threshold, the linen is ablated and/or vaporized, while when $F_T < 13$ J/cm$^2$ the linen does not change color. Even when $F_T$ is in the coloration range, not all the irradiated fibers are colored (Figs. 5 and 16) due to the spatial fluctuations of energy density of the laser pulses shown in Fig. 15.

III. We triggered a photochemical coloration process. In fact, the thermal heating associated with UV and VUV radiation is within a few degrees centigrade and therefore irrelevant for the purpose of coloring by scorching linens; see Fig. 13. This result fits with the "cold" coloration process of the Shroud estimated in [8,11,12].

IV. The hue of color depends on the wavelength and on the number $N$ of laser pulses, which is proportional to $F_T$. Irradiations at 0.308 μm generate a brownish coloration, while the 0.193 μm photons produce a yellow color (see Fig. 4) comparable to the color of the Shroud image. In both cases, the contrast slowly increases with the number of laser pulses, allowing an accurate control of the RGB value by varying $F_T$.

V. The different hue of color obtained by UV and VUV radiation is due to different chains of photochemical reactions respectively triggered. In particular, the VUV radiation at 0.193 μm is absorbed by alkene groups in degraded cellulose, whose number increases with $F_T$, thus inducing a photolysis of the cellulose, which promotes the formation of chromophores; see Fig. 14. These chromophores determine the yellow coloration of the fibers [8,12,39–41].

VI. We observed an irradiated fiber whose coloration was possibly confined in the primary cell wall [35,36], which is comparable with the thinnest coloration depth observed in the fibers image of the Shroud of Turin [8,11,19].

VII. Aging can be a concause of linen coloration. In fact, after laser irradiations that, at first, do not generate a visible coloration of linen, a latent coloration appears either by artificial (Fig. 8) or natural aging of linen [32,35]. Latent coloration is interesting for the synergy between UV, oxidation, and the dehydrating effect of heat (or of aging), which triggers the coloration process, and also for historians, attracted by the possibility that, whatever may have caused the Shroud image, the coloration may have developed over time.

VIII. The partial inhibition of fluorescence induced by VUV laser radiation (Fig. 9) is an additional feature of our coloration similar to the Shroud image. The induced fluorescence is also capable to selectively recognize the uniformity of $F_T$ incident on linen; see Figs. 9(a) and 9(b).

IX. Both UV and VUV radiations coloring linen are compatible with the absence of image under the bloodstains on the Shroud because in this spectral region light is absorbed by very thin layers of blood hemoglobin. According to [45] the UV light may be responsible for another special feature of the Shroud: the red color of blood stains after so much time since their deposition.

X. Using a petrographic microscope, we have observed some defects induced by UV radiation in the structure of irradiated linen fibers (see Fig. 12), similar to very old linen fabrics [11,46].

XI. Absolute reflectance measurements show that, when irradiated in the UV and VUV, our linen behaves like the linen of the Shroud; see Fig. 10.

In summary, our results demonstrate that a short and intense burst of directional VUV radiation can color a linen cloth so as to reproduce many of the peculiar characteristics of the image on the Shroud of Turin, including the hue of color, the shallow penetration depth of the color, and the inhibition of fluorescence.

The Shroud image has characteristics that we have been able to reproduce only in part, for example the gross shading structure that is determined by the ratio of yellow to uncolored fibers in a given area; see point (f) in Section 1 and Fig. 16. As discussed in Section 8.A, sophisticated diffractive optics could replicate these features, but this effort is far beyond our intention. In fact, our purpose was not to demonstrate that a battery of 10,000 lasers can accurately reproduce the image on the Shroud. Our main purpose was to perform accurate and reproducible experiments apt to understand the physical and chemical mechanisms that might have played a role in the generation of the Shroud body image, using a powerful and versatile tool such as the laser, regardless of the source of energy that may have caused this image. In this frame, our experimental data can be helpful to scholars seeking a linen coloration by corona discharge [18] or electrostatic discharge and radon emitted during seismic events [47], which involve UV and VUV light but are difficult to control and characterize.

This is not the conclusion; we are composing pieces of a fascinating and complex scientific puzzle. The enigma of the body image of the Shroud of Turin is still "a challenge to our intelligence" [48].

The authors thank Professor Giulio Fanti (University of Padua) for photomicrographs of fibers,

for photos of Fig. 13, and for useful discussions about the manuscript contents.

## References


1. G. Fanti, J. A. Botella, F. Crosilla, F. Lattarulo, N. Svensson, R. Schneider, and A. Wanger, "List of evidences of the Turin Shroud," in *Proceedings of the International Workshop on the Scientific Approch to the Acheiropoietos Images*, P. Di Lazzaro, ed. (ENEA, 2010), pp. 67–75, http://www.acheiropoietos.info/proceedings/proceedings.php.
2. B. J. Culliton, "The mystery of the Shroud challenges 20th-century science," Science **201**, 235–239 (1978).
3. R. Gilbert and M. Gilbert, "Ultraviolet visible reflectance and fluorescence spectra of the Shroud of Turin," Appl. Opt. **19**, 1930–1936 (1980).
4. E. J. Jumper and W. Mottern, "Scientific investigation of the Shroud of Turin," Appl. Opt. **19**, 1909–1912 (1980).
5. S. F. Pellicori, "Spectral properties of the Shroud of Turin," Appl. Opt. **19**, 1913–1920 (1980).
6. J. S. Accetta and J. S. Baumgart, "Infrared reflectance spectroscopy and thermographic investigations of the Shroud of Turin," Appl. Opt. **19**, 1921–1929 (1980).
7. R. A. Morris, L. A. Schwalbe, and J. R. London, "X-ray fluorescence investigation on the Shroud of Turin," X-Ray Spectrom. **9**, 40–47 (1980).
8. J. H. Heller and A. D. Adler, "A chemical investigation of the Shroud of Turin," Can. Soc. Forensic Sci. J. **14**, 81–103 (1981).
9. S. F. Pellicori and M. S. Evans, "The Shroud of Turin through the microscope," Archaeology **34**, 34–43 (1981).
10. V. D. Miller and S. F. Pellicori, "Ultraviolet fluorescence photography of the Shroud of Turin," J. Biol. Photogr. **49**, 71–85 (1981).
11. L. A. Schwalbe and R. N. Rogers, "Physics and chemistry of the Shroud of Turin, a summary of the 1978 investigation," Anal. Chim. Acta **135**, 3–49 (1982).
12. E. J. Jumper, A. D. Adler, J. P. Jackson, S. F. Pellicori, J. H. Heller, and J. R. Druzik, "A comprehensive examination of the various stains and images on the Shroud of Turin," in *Archaeological Chemistry III*, Vol. **205** of ACS Advances in Chemistry Series (American Chemical Society, 1984), pp. 447–476.
13. W. C. McCrone and C. Skirius, "Light microscopical study of the Shroud of Turin," Microscope **28**, 105–111 (1980).
14. J. P. Jackson, E. J. Jumper, and W. R. Ercoline, "Correlation of image intensity on the Turin Shroud with the 3-D structure of a human body shape," Appl. Opt. **23**, 2244–2270 (1984).
15. J. P. Jackson, "Is the image on the Shroud due to a process heretofore unknown to modern science?," Shroud Spectrum Int. **34**, 3–29 (1990).
16. T. Heimburger, "A detailed critical review of the chemical studies on the Turin Shroud: facts and interpretations," (2001), http://www.shroud.com/pdfs/thibault%20final%2001.pdf.
17. I. Piczek, "Is the Shroud of Turin a painting?," (1995), retrieved on 10 October 2012, http://www.shroud.com/piczek.htm.
18. G. Fanti, "Can corona discharge explain the body image of the Turin Shroud?," J. Imaging Sci. Technol. **54**, 020508 (2010).
19. G. Fanti, J. Botella, P. Di Lazzaro, R. Schneider, and N. Svensson, "Microscopic and macroscopic characteristics of the Shroud of Turin image superficiality," J. Imaging Sci. Technol. **54**, 040201 (2010).
20. L. Garlaschelli, "Life-size reproduction of the Shroud of Turin and its image," J. Imaging Sci. Technol. **54**, 040301 (2010).
21. F. Ferrero, F. Testore, C. Tonin, and R. Innocenti, "Surface degradation of linen textiles induced by laser treatment," AUTEX Res. J. **2**, 109–114 (2002).
22. S. Perez and K. Mazeau, *Polysaccharides: Structural Diversity and Functional Versatility*, S. Dumitriu, Ed. (Dekker, 2004), Chap. 2.
23. J. H. Heller and A. D. Adler, "Blood on the Shroud of Turin," Appl. Opt. **19**, 2742–2744 (1980).
24. P. L. Baima Bollone, "Indagini identificative su fili della Sindone," G. Accad. Med. Torino **1**, 228–239 (1982).
25. P. E. Damon, D. Donahue, B. Gore, A. Hatheway, A. Jull, T. Linick, P. Sercel, L. Toolin, C. Bronk, E. Hall, R. Hedges, R. Housley, I. Law, G. Bonani, S. Trumbore, W. Woelfli, J. Ambers, S. Bowman, M. Leese, and M. Tite, "Radiocarbon dating of the Shroud of Turin," Nature **337**, 611–615 (1989).
26. R. Van Haelst, "A critical review of the radiocarbon dating of the Shroud of Turin," in *Proceedings of the International Workshop on the Scientific Approach to the Acheiropoietos Images*, P. Di Lazzaro, ed. (ENEA, 2010), pp. 267–273, http://www.acheiropoietos.info/proceedings/proceedings.php.
27. R. N. Rogers, "Studies on the radiocarbon sample from the Shroud of Turin," Thermochim. Acta **425**, 189–194 (2005).
28. D. Scavone, "Documenting the Shroud's missing years," in *Proceedings of the International Workshop on the Scientific Approach to the Acheiropoietos Images*, P. Di Lazzaro, ed. (ENEA, 2010), pp. 87–94, http://www.acheiropoietos.info/proceedings/proceedings.php.
29. A. Nicolotti, *I Templari e la Sindone. Storia di un falso* (Salerno, 2011), Chaps. 1, 3, and 4.
30. N. Svensson, "Medical and forensic aspects on the man depicted on the Shroud of Turin," in *Proceedings of the International Workshop on the Scientific Approach to the Acheiropoietos Images*, P. Di Lazzaro, ed. (ENEA, 2010), pp. 181–186, http://www.acheiropoietos.info/proceedings/proceedings.php.
31. G. Baldacchini, P. Di Lazzaro, D. Murra, and G. Fanti, "Colorazione di tessuti di lino con laser ad eccimeri e confronto con l'immagine sindonica," Technical Report ENEA RT/2006/70/FIM (ENEA, 2006).
32. G. Baldacchini, P. Di Lazzaro, D. Murra, and G. Fanti, "Coloring linens with excimer lasers to simulate the body image of the Turin Shroud," Appl. Opt. **47**, 1278–1285 (2008).
33. P. Di Lazzaro, G. Baldacchini, G. Fanti, D. Murra, and A. Santoni, "Colouring fabrics with excimer lasers to simulate encoded images: the case of the Shroud of Turin," Proc. SPIE **7131**, 71311R (2009).
34. P. Di Lazzaro, G. Baldacchini, G. Fanti, D. Murra, E. Nichelatti, and A. Santoni, "A physical hypothesis on the origin of the body image embedded into the Turin Shroud," in *Proceedings of the International Conference on the Shroud of Turin: Perspectives on a Multifaceted Enigma*, G. Fanti ed. (Libreria Progetto Padova, 2009), pp. 116–125, http://www.ohioshroudconference.com/papers/p01.pdf.
35. P. Di Lazzaro, D. Murra, A. Santoni, G. Fanti, E. Nichelatti, and G. Baldacchini, "Deep ultraviolet radiation simulates the Turin Shroud image," J. Imaging Sci. Technol. **54**, 040302 (2010).
36. P. Di Lazzaro, D. Murra, A. Santoni, and G. Baldacchini, "Sub-micrometer coloration depth of linens by vacuum ultraviolet radiation," in *Proceedings of the International Workshop on the Scientific Approach to the Acheiropoietos Images*, P. Di Lazzaro, ed. (ENEA, 2010), pp. 3–10, http://www.acheiropoietos.info/proceedings/proceedings.php.
37. P. Di Lazzaro, D. Murra, A. Santoni, and G. Baldacchini, "Colorazione simil-sindonica di tessuti di lino tramite radiazione nel lontano ultravioletto," Technical Report ENEA RT/2011/14/ENEA (ENEA, 2011), retrieved 10 October 2012, http://opac.bologna.enea.it:8991/RT/2011/2011_14_ENEA.pdf.
38. http://www.perkinelmer.com/CMSResources/Images/44-74789SPC_LAMBDA1050LAMBDA950.pdf, retrieved 10 October 2012.
39. G. Novelli, "La Sindone e la scienza chimica," in *Proceedings of the Worldwide Congress Sindone 2000*, A. Russi and E. Marinelli, eds. (Gerni, 2002), pp. 175–181.
40. A. Mosca Conte, O. Pulci, A. Knapik, J. Bagniuk, R. Del Sole, J. Lojewska, and M. Missori, "Role of cellulose oxidation in the yellowing of ancient paper," Phys. Rev. Lett. **108**, 158301 (2012).
41. A. Bos, "The UV spectra of cellulose and some model compounds," J. Appl. Polym. Sci. **16**, 2567–2576 (1972).
42. M. Yatagai and S. H. Zeronian, "Effect of ultraviolet light and heat on the properties of cotton cellulose," Cellulose **1**, 205–214 (1994).

43. See, e.g., F. Gori, "Diffractive optics, an introduction," in *Diffractive Optics and Optical Microsystems*, S. Martellucci and A. N. Chester, eds. (Plenum, 1997), pp. 3–23.
44. R. N. Rogers, "Testing the Jackson 'theory' of image formation," (2004), retrieved 10 October 2012, http://www.shroud.com/pdfs/rogers6.pdf.
45. C. Goldoni, "The Shroud of Turin and the bilirubin blood stains," in *Proceedings of the International Conference on the Shroud of Turin: Perspectives on a Multifaceted Enigma*, G. Fanti, ed. (Libreria Progetto Padova, 2009), pp. 442–445, http://www.ohioshroudconference.com/papers/p04.pdf.
46. R. N. Rogers, "The Shroud of Turin: radiation effects, aging and image formation," (2005), retrieved 10 October 2012, http://www.shroud.com/pdfs/rogers8.pdf.
47. G. De Liso, "Shroud-like experimental image formation during seismic activity," in *Proceedings of the International Workshop on the Scientific Approach to the Acheiropoietos Images*, P. Di Lazzaro, ed. (ENEA, 2010), pp. 11–18, http://www.acheiropoietos.info/proceedings/proceedings.php.
48. Pope John Paul II, "The Shroud is a challenge to our intelligence," address during the visit to Turin (24 May 1998).